

# Research on the Mechanical Design of Two-Axis Fast Steering Mirror for Optical Beam Guidance

Hany F. Mokbel

College of Mechanical and Electric Engineering,  
Changchun University of Science and Technology  
Changchun, Jilin, China

Wan Yuan

College of Mechanical and Electric Engineering,  
Changchun University of Science and Technology  
Changchun, Jilin, China

Lv Qiong Ying

College of Mechanical and Electric  
Engineering,  
Changchun University of Science and  
Technology  
Changchun, Jilin, China

Cao Guo Hua

College of Mechanical and Electric  
Engineering,  
Changchun University of Science and  
Technology  
Changchun, Jilin, China

Amr A. Roshdy

College of Mechanical and Electric  
Engineering,  
Changchun University of Science and  
Technology  
Changchun, Jilin, China

**Abstract**—In this work, Two-Axis Fast Steering Mirror (*FSM*) was designed to facilitate the fast and precise positioning for an optical bundle of a Three Dimensional (*3D*) scanner consists mainly of a Laser Range Finder (*LRF*) and a Complementary Metal–Oxide–Semiconductor (*CMOS*) camera. The *FSM* system architecture, mirror structure, compliant mechanisms' design, and actuators' selection were discussed in details. Meanwhile, the system analysis results were clearly depicted based on *3D* solid modeling and Finite Element Method (*FEM*) analysis. The *FSM* design was designed to achieve a clear elliptical optical aperture of  $2 \times 3$  inch, bandwidth of  $1 \text{ KHz}$ , and an optical rotational angle of  $\pm 2 \text{ mrad}$ . Finally, a general discussion for the *FSM* system enhancement was introduced for further optimization processes.

**Keywords**- Fast Steering Mirror (*FSM*); Finite Element Method (*FEM*); Compliant Mechanisms

## I. INTRODUCTION

For the purpose of directing the Line Of Sight (*LOS*) of Electro-Optical (*EO*) devices two methods are commonly used, namely; the mass stabilization and the mirror stabilization [1]. In the  $1^{st}$  method, the massive *EO* devices perform the required rotations about one, two, or three axes through the same number of gimbals; of course increasing the number of gimbals will increase the volume and mass of the whole system [2 & 3]. This method can achieve wide range of rotations and even a continuous  $360^\circ$  in the required direction. Due to the massive structure and the consequently high inertia, the angular rates, accelerations, bandwidth, response, and settling time are usually limited to certain values [4]. In the  $2^{nd}$  method, Mirror stabilization, the *EO* devices are connected to a fixed platform, while the optical beams falls on the reflecting surface of Fast Steering Mirror (*FSM*) with predetermined incident angle to reflect on this surface with the same incident angle to reach the target point. By changing the angular position of the *FSM*, the position of the optical beam will also change by twice the mechanical angle [5]. This method can achieve very high

bandwidths due to the low inertia of the rotating masses, high accelerations and angular rate, higher precisions, fast response and settling times [6 & 7]. But, on the other hand they have limited angular rotations in the range of few mille radians, or in the best cases, few degrees on the account of decreasing the band width [8]. *FSM* have become key components in diverse applications in both the civilian and military fields such as industrial instrumentation, astronomy, optical communication, and imaging systems [9]. The early *FSM* was a single mirror driven by a galvanometer to rotate around one axis. The use of two single axis mirrors can achieve the two axes operation required in so many applications. The galvanometer is an electromagnetic actuator that can achieve high angular rotation up to tens of degrees, but with limited bandwidth. On the contrary, piezoelectric actuators can drive the mirrors with low angular travel in the range of few mille radians, but with higher stiffness and bandwidth. Other widely used mirrors' driving actuators are the voice coil actuators (mostly similar to the galvanometer, but it provides linear force in stead of the torque). The average size of the commercial *FSM* ranges from several millimeters up to tens of millimeters, and the bandwidth several Hertz to hundreds of Hertz. Notably, the tradeoff between increasing the mirror size and the achieved bandwidth has been taking a lot of concern from many researchers.

## II. FSM SYSTEM ARCHITECTURE

The *FSM* system architecture shown in *Fig.1* consists mainly from the mirror body that fabricated from one piece of aluminum substrate with silver coated reflecting surface, and an elliptical clear aperture of  $2 \times 3$  inch. The system features four piezoelectric actuators; each pair of actuators operates in a push-pull mode to rotate the mirror around one axis.

The piezoelectric actuators are of the type *P-841.1B* preloaded piezo actuators from *PI* with an integrated high-resolution strain gauge position sensor for high precision closed loop operation. In the heart of the *FSM* there exists the

compliant axial flexure that provides the compliant two rotational degrees of freedom to the *FSM* while it constrains the linear translation along the *X*-axis. As shown in Fig.2, the rotation of the *FSM* by a mechanical angle  $\alpha$ , results in a change of the reflected beam optical angle of  $2\alpha$ .

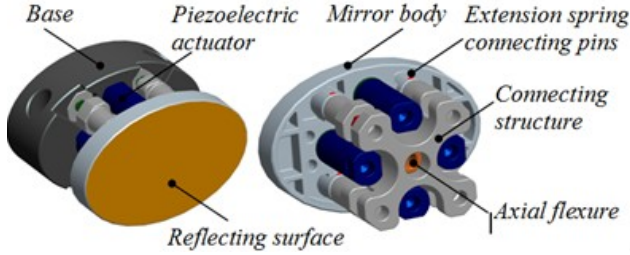


Figure 1. The FSM system architecture.

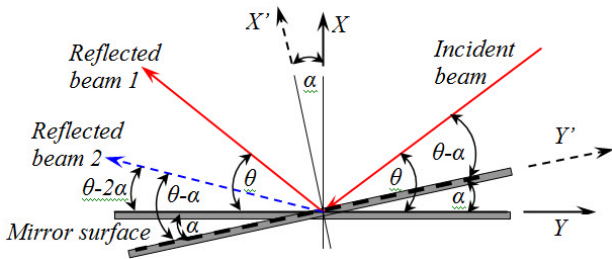


Figure 2. The rotation of the FSM about the Z-axis by a mechanical angle  $\alpha$ , results in a change of the reflected beam optical angle of  $2\alpha$ .

Four compliant preloaded high stiffness springs are used to assure the continuous attachment of the mirror body to the actuators tip surfaces as well as to counteract the effect of gravitational forces on the *FSM* body for harsh operating conditions. The smart design of the *FSM* connecting structure facilitates the ease of the assembly and disassembly of the Mirror body, piezoelectric actuators, and compliant mechanisms to the *FSM* base plate, in the same time; it provides additional stiffness to the whole vibrating mechanism. Meanwhile, the *FSM* components are all assembled to a massive base which represents the fixed platform. Moreover, the base can be attached to a supplementary base, shown in Fig.7 to provide more flexibility to the *FSM* system presetting.

#### A. Mechanical Design and Control System Considerations

The Opto-Electro-Mechanical system design of *FSM* involves many disciplines. Of them, the mechanical design is responsible for the whole system performance. For instance, in a laser pointing system, the precision of the laser beam direction, the beam acceleration and stability are all determined in terms of the characteristics of the mechanical system. Also, the system bandwidth, in most cases, is limited to the mechanical system bandwidth, which raises the urgent requirement to increase the mechanical system bandwidth. Moreover, for making the mechanical design controllable, it is always preferred to design a mechanical system that decouples the effect of rotation about each axis, to facilitate the use of the Single-Input/Single-Output (*SISO*) controller independently for each axis. Herein, the mechanical design was completed and optimized by the aid of the *Pro/Engineer 3D CAD* software and the *ANSYS FEM* analysis software. In order to solve the

problem of decoupling, the vibrating mirror body was designed to be symmetric about each axis of rotation and the geometric center of rotation is aligned with the center of mass.

#### B. Mirror Design

Many different materials are available for the manufacturing of the mirrors; the optimum choice of the stiffness to mass ratio is the governing factor for the material selection. In general, to obtain a high bandwidth, stable performance and high response *FSM*, it is desirable to have a low inertia mirror structure by choosing a low density and high modulus of elasticity for the mirror's material, as well as increasing the stiffness of the mirror body structure. Unfortunately, increasing the stiffness of the mirror structure, by increasing its thickness, to withstand the high reciprocating natural, will increase the inertia forces and decreases the whole system bandwidth. This tradeoff between inertia and stiffness is a crucial point in the design process. In this research, the *EO* devices have an optical bundle of 65 mm in width and 30 mm in height. The mirror was fabricated from one piece of Aluminum, with a large optical aperture of 50 X 75 mm elliptical protected silver coated Aluminum mirror substrate. The reflected wave front error is  $\lambda/900$  Root Mean Square (*RMS*) and  $\lambda/250$  Peak-to-Valley (*P-V*) at 632 nm wavelength.

#### C. Piezoelectric Actuators

Many advantages of the piezoelectric actuators over the conventional Electromagnetic motors and Voice-coil motors are depicted in many articles. Piezoelectric motors have high power to size ratio, high holding force at zero power input, low inertia, fast start and stop, not affected by electromagnetic fields, non accompanying electromagnetic field, silent drive, Nano and sub Micrometer positioning. On the other hand, there are some disadvantages in the use of piezoelectric motors such as the need for amplifiers to produce the high voltage and high frequency power needed for driving the piezo motor. Herein, the preloaded piezo actuators type *P-841.1B* have an integrated high-resolution strain gauge position sensors provides high precision for closed loop operation (*2msec settling time to a 3nm peak to peak square wave input signal of 240 Hz*) and resolution of 0.3 nm. They have a 15μm Travel Range, Pushing Forces to 1000 N, Pulling Forces to 50 N, unloaded resonant frequency of 18 KHz.

#### D. Compliant Mechanisms

The *FSM* is required to rotate about the *Y* and *Z*-axes, ( $\psi$  and  $\alpha$ ), while it must be constrained in the other four Degrees of Freedom (*DOF*) (*Rotation about X-axis and translation in the three axial directions*). Two kinds of compliant mechanisms are used to achieve these constraints while keeping compliance in the required 2 *DOF*.

##### 1) Axial Flexure Design

The Axial Flexure is used to provide a pivoting point to the *FSM*. Meanwhile, it constrains the *FSM* in the  $-X$  direction. The axial flexure design must withstand the axial load and buckling, while, permits the bending in the lateral direction to achieve the designed mirror's rotations. This means the flexure must have high axial and torsional stiffness while keeping a

lower stiffness in bending. From (1, 2, 3, and 4) for the axial, bending, torsional stiffness, and the critical force for buckling ( $k_{ax}$ ,  $k_{be}$ ,  $k_t$ , and  $F_{cr}$ ) respectively, it is clear that the design is directed to maximize the area of the axial flexure as possible with a keeping the area moment of inertia as minimum as possible. Where Cross-sectional area ( $A = \pi d^2/4$ ) ( $mm^2$ ), ( $E$ ) Modulus of Elasticity ( $GPa$ ), ( $G$ ) Modulus of Rigidity ( $GPa$ ), ( $L$ ) Flexure length (mm), Area moment of inertia ( $I = \pi d^4/64$ ) ( $mm^4$ ), and the Polar moment of inertia ( $J = \pi d^4/32$ ) ( $mm^4$ ).

$$k_{ax} = AE/L \quad (1)$$

$$k_{be} = IE/L \quad (2)$$

$$k_t = JG/L \quad (3)$$

$$F_{cr} = \pi^2 EI/L^2 \quad (4)$$

Due to the *FSM* architecture, the actuators act in a push/pull manner that pivots on the axial flexure tip, in the ideal case there will not be any axial force on the axial flexure. Practically, the only axial force on the axial flexure will arise from the mismatch of the actuators' forces. So, the design was made to withstand a mismatch of 5% of the actuators maximum force, which is 50 N. The material of the axial flexure was chosen to be a commonly used stainless steel *S17400* commercially available under the name of *AL 17-4* alloy. It has a Modulus of Elasticity of 196GPa and a Modulus of Rigidity of 77.2GPa. The flexure was designed to undergo a deflection of 1μm due to an applied force of 50N, which means a stiffness of 50X10<sup>3</sup> N/mm. Using (1, 2, and 3) with simple iterations it can be found that the optimal dimensions for the flexure shown in Fig.3 are diameter ( $d=3mm$ ), and length ( $L=20mm$ ) that provides axial stiffness of 69.3X10<sup>3</sup> N/mm, bending stiffness of 38.97X10<sup>3</sup> N/mm, and torsional stiffness of 30.97X10<sup>3</sup> N/mm which achieves the goals of the flexure design. Moreover checking for the buckling using (4) showing the ability of the axial flexure to prevent buckling due to the axial forces. Finally, the steel material for the axial flexure insures an infinite fatigue life for the flexure.



Figure 3. The Axial Flexure and Extension Spring mechanisms.

## 2) Extension Spring

Four preloaded extension springs are used to attach the mirror body to the *FSM* mechanism. Where, the preload prevents the movement of the mirror body due to the gravitational forces. Meanwhile, the springs were designed to facilitate a working frequency of 1 KHz. Using (5 & 6) for the natural frequency of the spring ( $f_s$ ), and substituting for the effective mass on each spring ( $m_s$ ), we can get the required spring stiffness ( $k_s$ ). Ultimately, the extension spring was designed to have a wire diameter ( $d_s$ ) of 2mm, mean spring diameter ( $D_s$ ) of 4mm, Shear modulus ( $G$ ) of 79GPa, and four active coils ( $N_s$ ).

$$f_s = (1/2\pi)\sqrt{k_s/m_s} \quad (5)$$

$$k_s = d_s^4 G / 8 D_s^3 N_s \quad (6)$$

## III. SYSTEM ANALYSIS

The most critical component of the *FSM* system is the mirror body itself, where any deformation in the reflecting surface will affect the optical beam guidance. So, the mirror body was comprehensively tested and optimized. Since the *FSM* working principle depends on the high resonating nature of the system, it was important to start with testing the resonance frequency of the mirror body. In all the following analysis, the normal direction to the mirror surface represents the *X*-axis as shown in Fig.2, and the other two axes are parallel the mirror surface, and hence, the primary modes of concern will be the bending modes along the *Y* and *Z* axes. The mirror body was tested for the first five modes of Natural Frequency, the 1<sup>st</sup> mode of vibration appears at 19285 Hz which is bending about the *Z*-axis, followed by the 2<sup>nd</sup> bending mode about the *-Z*-axis. The first 5 modes of vibration results appear in Fig.4 and Table 1. It is clear that the stiff and light weight mirror structure have obtained high values for the natural frequencies that afford high working bandwidth.

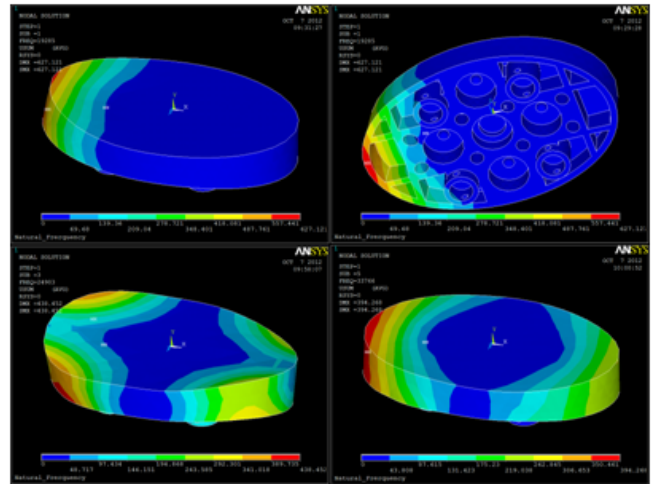


Figure 4. Frontal and back view of the 1<sup>st</sup> mode of vibration of the mirror body (upper row), the 3<sup>rd</sup> and 5<sup>th</sup> modes (Lower row).

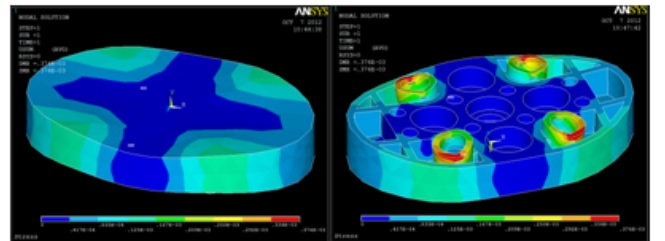


Figure 5. Frontal and back view of the deflection analysis on the mirror body.

Furthermore, the mirror body was tested for deflections due to stresses from the preloaded extension springs and the gravitational force. The Maximum deflection was found to be 376 nm on the back surface, as shown in Fig.5 where the four extension springs are mounted, while the maximum deflection

on the frontal mirror surface hardly reaches  $167\text{ nm}$  on the far edges of the mirror, and in most of the reflecting surface are normally less than  $40\text{ nm}$ . The maximum stresses were found to be  $4.626\text{ MPa}$  on the back surface and  $0.5\text{ MPa}$  on the frontal surface. Finally, The Piezoelectric actuators were manufactured to have  $18\text{ KHz}$  unloaded resonant frequency. But as a result to the implementation of these actuators into the working system, it is expected that the Natural modes of vibration will be reduced. The *FEM* modal analysis of the actuators simulated a  $1^{\text{st}}$  mode of vibration at  $7493\text{ Hz}$ . Accordingly, these results will be reduced more when testing the actuators with the mirror as one system, in this case, the  $1^{\text{st}}$  mode of natural frequency of this subsystem has reached  $3369\text{ Hz}$ . The *FEM* modal analysis and the results for these two cases, the modal analysis for the axial flexure and the connecting structure along with the whole *FSM* model are all depicted in *Fig.6* and *Table 1*.

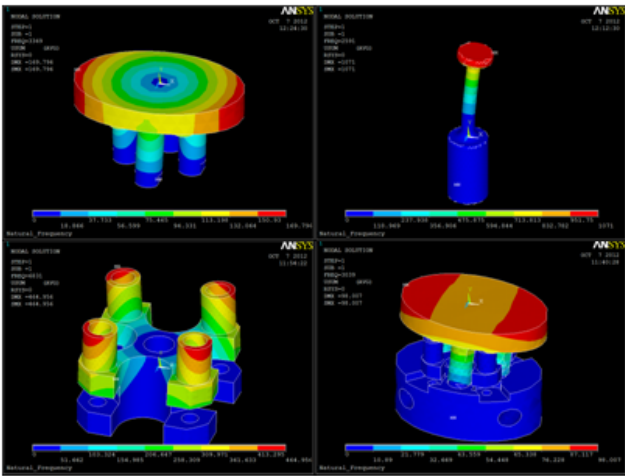


Figure 6. FEM modal analysis of the different FSM system components.

TABLE I. THE FIRST FIVE MODES OF NATURAL FREQUENCY FOR THE DIFFERENT COMPONENTS OF THE FSM

Mode No.	Tested component				
	Mirror structure	Actuator	Mirror + Actuators	Axial flexure	Connecting structure
1	19285	7493	3369	2591	6831
2	19590	8074	3423	2624	7564
3	24903	27349	3616	11733	7892
4	25198	36658	8984	20137	7897
5	33766	37152	10233	20460	11088

#### IV. DISCUSSION AND OPTIMIZATION

In a lumped mass-spring system (Like that one of the *FSM* system) the modes of vibration of the individual components will completely differ from that of the subsystems or the whole system. Where, the assembling of two components together will result in a new subsystem that have a new mass, stiffness, and natural vibration modes higher or lower than that of the original ones. For this reason and of course the possibility of manufacturing and assembling inaccuracies and the added masses from cables and connectors, and also the preloading, linear and nonlinear friction and cables restraints forces, and many other actual working conditions, the design goal was set

to only  $1\text{ KHz}$  operating bandwidth although the results of the *FSM* can achieve  $3\text{ KHz}$  bandwidth.

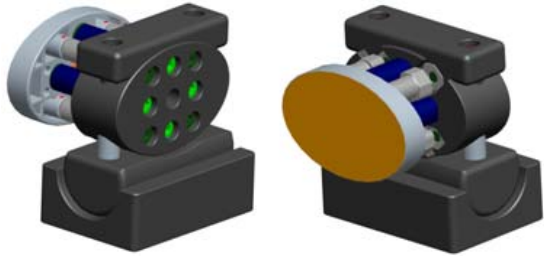


Figure 7. The *FSM* system with the supplementary base.

Increasing the mechanical angle from  $\pm 1\text{ mrad}$  to  $\pm 3\text{ mrad}$  by increasing the linear travel of the piezoelectric actuators from  $15\mu\text{m}$  to  $45\mu\text{m}$  will dramatically decrease the *FSM* system bandwidth from  $1\text{ KHz}$  to about  $0.6\text{ KHz}$ . For the same *FSM* system architecture but replacing the Aluminum mirror substrate with a Beryllium one, will decrease the mirror mass from  $64\text{ gm}$  to about  $40\text{ gm}$  and increase the *FSM* system bandwidth from  $1\text{ KHz}$  to  $1.2\text{ KHz}$ . The flexible design of the *FSM* supplementary base shown in *Fig.7* facilitates the pre-orientation of the *FSM* in several directions without loosing the designed system stiffness. Stiffen the area around the extension spring mounting in the back surface of the mirror body will decrease the deflection of the frontal mirror surface from  $40\text{ nm}$  to less than  $10\text{ nm}$ .

#### V. CONCLUSION

*FSM* are used in application requiring high bandwidth, fast and precise optical beam guidance. Piezoelectric actuators are commonly used in these systems to achieve higher bandwidths, quick response, accurate positioning, minimal step, small size, but on the expense of the low linear travel or rotation angle. The use of compliant mechanisms such as the axial flexure facilitates the achievement of high resonating pivoting without any friction losses. The use of both the *3D* solid modeling and the *FEM* analysis in an iterative feedback design procedures is an effective way in Mechanical systems integration of the *FSM*. The tradeoffs between the optical aperture size, system inertia, bandwidth, stiffness, and the available rotation angle are of great important in *FSM* system design. The designed *FSM* has achieved an elliptical optical aperture of  $75 \times 50\text{ mm}$ , and has proved to simulate a working bandwidth of  $3\text{ KHz}$ , with an optical rotation angle of  $\pm 2\text{ mrad}$ . Further enhancement to the *FSM* system can be achieved by utilizing a lighter and stiffer mirror substrate like Beryllium that can achieve  $20\%$  higher bandwidth for the same designed system.

#### REFERENCES

- [1] M. K. Masten, "Inertially stabilized platforms for optical imaging systems", *IEEE Control Systems Magazine*, Vol. 28, pp. 47–64, 2008.
- [2] H. F. Mokbel, L. Q. Ying, A. A. Roshdy, and C. G. Hua, "Design optimization of the inner gimbal for dual axis inertially stabilized platform using finite element modal analysis", *International Journal of Modern Engineering Research*, Vol.2, pp. 239-244, 2012.
- [3] Z. X. yang, Y. Ruixia, L. J. ping, and L. Dapeng, "Structure optimal design of roll gimbal for an aerial three-axis ISP based on FEM modal analysis" *3<sup>rd</sup> International Conference on Measuring Technology and Mechatronics Automation*, Vol. 3, pp. 373 – 376, 2011.

- [4] H. F. Mokbel, L. Q. Ying, A. A. Roshdy, and C. G. Hua, "Modeling and optimization of electro-optical dual axis inertially stabilized platform", International Conference on Optoelectronics and Microelectronics, pp. 372-377, 2012.
- [5] Q. Zhou, P. Ben-Tzvi, D. Fan, and A. A. Goldenberg, "Design of fast steering mirror systems for precision laser beams steering", IEEE International Workshop on Robotic and Sensors Environments, 2008.
- [6] D. J. Kluk, M. T. Boulet, and D. L. Trumper, "A high-bandwidth, high precision, two-axis steering mirror with moving iron actuator", Mechatronics, Vol. 22, pp. 257-270, 2012.
- [7] F. M. Taposa, et al, "High bandwidth fast steering mirror", Optomechanics 2005, , Proceedings of SPIE Vol. 5877, 2005.
- [8] S. Woody, and S. Smith, "Design and performance of a dual drive system for tip-tilt angular control of a 300 mm diameter mirror", Mechatronics, Vol. 16, pp. 389-397, 2006.
- [9] Kluk D. J., An advanced fast steering mirror for optical communications, M.S. Thesis, Massachusetts Institute of Technology, 2007.